Heliyon 10 (2024) e27329

Contents lists available at ScienceDirect

Heliyon

journal homepage: www.cell.com/heliyon

Research article

Tumor-infiltrating CD8$^+$ sub-populations in primary and recurrent glioblastoma: An *in-silico* study

Mahdi Abdoli Shadbad [a,b,1,*], Adib Miraki Feriz [c,d,1], Behzad Baradaran [b,e], Hossein Safarpour [d,**]

[a] Student Research Committee, Tabriz University of Medical Sciences, Tabriz, Iran
[b] Immunology Research Center, Tabriz University of Medical Sciences, Tabriz, Iran
[c] Student Research Committee, Birjand University of Medical Sciences, Birjand, Iran
[d] Cellular and Molecular Research Center, Birjand University of Medical Sciences, Birjand, Iran
[e] Department of Immunology, Faculty of Medicine, Tabriz University of Medical Sciences, Tabriz, Iran

ARTICLE INFO

Keywords:
Glioblastoma
CD8 lymphocytes
Single-cell RNA sequencing
Immune checkpoint

ABSTRACT

Background: Glioblastoma multiforme (GBM) remains an incurable primary brain tumor. CD8$^+$ tumor-infiltrating lymphocytes (TILs) can target malignant cells; however, their anti-tumoral immune responses mostly do not lead to GBM rejection in GBM patients. We profiled the sub-populations of tumor-infiltrating CD8$^+$ T-cells, i.e., naïve, cytotoxic, and exhausted cells, in primary and recurrent GBM tissues and provided a blueprint for future precision-based GBM immunotherapy.

Method: We re-analyzed the raw data of single-cell RNA sequencing on the cells residing in the GBM microenvironment and leveraged tumor bulk RNA analyses to study the significance of CD8$^+$ TILs sub-populations in primary and recurrent GBM. We investigated cell-cell interaction between exhausted CD8$^+$ TILs and other immune cells residing in the primary and recurrent GBM microenvironments and profiled the expression changes following CD8$^+$ TILs' transition from primary GBM to recurrent GBM.

Results: Exhausted CD8$^+$ TILs are the majority of CD8$^+$ TILs sub-populations in primary and recurrent GBM, and cytotoxic CD8$^+$ TILs display decreased expression of inhibitory immune checkpoint (IC) molecules in the primary and recurrent GBM. In the primary and recurrent GBM microenvironment, exhausted CD8$^+$ TILs interact most with tumor-infiltrating dendritic cells.

Conclusion: This study demonstrates the profiles of CD8$^+$ TILs sub-populations in primary and recurrent GBM and provides a proof-of-concept for future precision-based GBM immunotherapy.

1. Introduction

Glioma is a common primary malignancy of the brain; glioblastoma multiforme (GBM) is the most aggressive type of glioma [1]. GBM has the highest mortality rate and the lowest 5-year survival rate; some issues hinder GBM treatment, including [1] the diverse nature of tumors, both within and between patients, and [2] the relatively impermeable blood-brain barrier, which inhibits the

* Corresponding author. Student Research Committee, Tabriz University of Medical Sciences, Tabriz, Iran.
** Corresponding author.
E-mail addresses: abdolim@tbzmed.ac.ir (M. Abdoli Shadbad), H.safarpour@bums.ac.ir (H. Safarpour).
[1] Co-first authors: These authors contributed equally to this work.

https://doi.org/10.1016/j.heliyon.2024.e27329
Received 23 October 2023; Received in revised form 26 February 2024; Accepted 28 February 2024
Available online 4 March 2024

efficient administration of many common treatments [2].

Immunotherapy is a new approach to treating some types of tumors. One of the main goals of cancer immunotherapy is to stimulate anti-tumoral immune responses [3]. $CD8^+$ tumor-infiltrating lymphocytes (TILs) can potentially target tumor cells; the T-cell receptor (TCR)-antigen-major histocompatibility complex (MHC)-I, along with co-stimulatory signal and pro-inflammatory factors, is needed to stimulate $CD8^+$ T-cell-mediated anti-tumoral immune responses [4,5]. $CD8^+$ TILs can be categorized into three main functional groups, i.e., naïve, cytotoxic, and exhausted $CD8^+$ TILs [6]. When $CD8^+$ T-cells encounter foreign antigens, they often differentiate into cytotoxic cells and control the progression of neoplasm or infection. However, these cells develop an "exhausted" phenotype during persistent exposure to foreign antigens. Recent findings have indicated that aberrant inhibitory immune checkpoint (IC) expression is associated with this dysfunctional phenotype [7]. Growing evidence has indicated that the pathological expression of inhibitory ICs can contribute to immune evasion and the development of immunosuppressive tumor microenvironment (TME) in solid cancers [8]. Targeting these ICs was thought to be an effective approach for stimulating anti-tumoral immune responses against GBM; nevertheless, it has been reported that administrating monoclonal antibodies (mAbs) against one or two of these ICs does not improve the survival of GBM patients [9].

Vast intra- and inter-tumoral heterogeneity can be reflected in why some affected patients respond to inhibitory IC blockade and others do not. The different expression profiles of inhibitory ICs among patients can be the culprit for the undesirable response of patients to specific IC inhibitors. Also, it has been suggested that there is a network of inhibitory ICs in the TME, and targeting one inhibitory axis might be insufficient to stimulate anti-tumoral immune responses; the compensatory roles of other inhibitory ICs can maintain pathological tolerance against tumoral cells [10]. Therefore, targeting a panel of inhibitory ICs might be sufficient to stimulate immune responses.

The advent of single-cell sequencing tools has presented several opportunities to investigate the expression patterns of individual cells. Implementing this technique in cancer biology has provided remarkable insights into the characteristics of different cell subpopulations inside tumor masses [11]. Single-cell sequencing techniques can aid in studying the expression profile of inhibitory ICs and provide insights into the underlying causes for the less-than-ideal outcomes seen in the present strategy of inhibitory IC blockage for afflicted individuals [10,12]. This study aimed to analyze the different subsets of $CD8^+$ TILs, crucial cells in both primary and recurrent GBM, and investigate the expression of well-known inhibitory ICs in these subsets. Furthermore, bioinformatics in this context furnishes unprecedented information regarding the mRNA expression profiles of $CD8^+$ TIL subpopulations as they progress from primary to recurrent GBMs, potentially offering prognostic significance for patient outcomes. Integrating bioinformatics is thus indispensable in unraveling the complexities of single-cell data and advancing our comprehension of cancer progression and treatment responses [13,14]. To the best of our knowledge, this is the first study thoroughly investigating subpopulations of $CD8^+$ TILs in primary and recurrent GBM and their interaction with other TME-residing cells. Besides studying the expression of well-known inhibitory ICs, this is the first study that comprehensively investigated the expression profile of $CD8^+$ TIL subpopulations in the progression from primary to recurrent GBMs.

2. Methods

2.1. Single-cell RNA sequencing analyses

2.1.1. Data acquisition

The raw data of GBM samples were obtained from the study by Abdelfattah et al. [15] under the GSE182109 accession number (https://www.ncbi.nlm.nih.gov/geo/). This study performed single-cell RNA sequencing on the primary and recurrent GBM tissues. The gene expression omnibus (GEO) expression matrix was annotated with gene symbols using information from the GPL20301 Illumina HiSeq 4000 (Illumina, San Diego, CA, USA). Data analysis was carried out using the Scanpy pipeline.

2.1.2. Quality control, dimensionality reduction, clustering, and visualization

We performed quality control to exclude low-quality cells; we only included the cells that contained [1] more than 500 genes [2], fewer than 17,500 counts, and [3] less than 20% of reads mapped to mitochondrial genes. Normalized expression was performed in Scanpy using the *normalize_total* function or by estimating size factors for each cell to minimize bias within cell counts and enhance intercellular comparability of cell expression levels. Dimensionality reduction was conducted on the top 4000 most highly variable genes to enable unsupervised grouping and cell-type identification using principal component analysis (PCA). In the next step, Louvain community detection, with a resolution of 0.5, was embedded into a k-nearest-neighbor graph. The expression levels of marker genes used for cell annotation. The markers for annotating $CD8^+$ TILs were adopted from the previous study [6]. Afterward, we created uniform manifold approximation and projection (UMAP) embeddings to visualize the most relative neighbor graph using a minimum distance of 0.5 and a spread of 1.0.

2.1.3. Cell-cell interaction

For studying cell-cell interaction, we utilized SquidPy, which provides analytic methods for storing, manipulating, and interactively visualizing single-cell RNA sequencing data. It employs an efficient re-implementation of the CellPhoneDB method capable of handling a high number of interacting pairs (100k+) and cluster combinations (100+).

2.1.4. Identifying differentially expressed genes (DEGs) between related $CD8^+$ TILs and enrichment analyses

We aimed to find the DEGs between the naïve, cytotoxic, and exhausted $CD8^+$ TILs in primary GBM and their counterpart

subpopulation in recurrent GBM. For this purpose, we applied the genes that met the following criteria: adjusted p-value < 0.05 and $|\text{fold change}| \geq 15$. Benjamini-Hochberg was used for adjusting the p-value. After identifying DEGs in $CD8^+$ T cell subpopulations, we used gene ontology analysis to study the molecular function of the identified DEGs. Bioinformatics (http://www.bioinformatics.com.cn/) was used for visualization.

2.2. RNA-sequencing on tumor bulk

2.2.1. The prognostic values of $CD8^+$ TILs subpopulations in primary GBM

The Survival Genie (https://bbisr.shinyapps.winship.emory.edu/SurvivalGenie/) was used to investigate the prognostic values of $CD8^+$ TILs subpopulations in primary GBM based on The Cancer Genome Atlas (TCGA)-GBM. This database enabled us to investigate the prognostic values of cell signatures in TCGA-GBM and confirm cell-type-specific marker genes derived from single-cell RNA sequencing.

2.2.2. Prognostic value of identified top DEGs for recurrent GBM patients

Because the number of included patients with recurrent GBM in the TCGA-GBM dataset was relatively low, we accessed the Chinese Glioma Genome Atlas (CCGA) dataset (http://www.cgga.org.cn/) to study the prognostic values of the identified DEGs for recurrent GBM patients.

2.2.3. The correlational study between inhibitory ICs in primary and recurrent GBM

We used the cBioPortal (https://www.cbioportal.org/) to access TCGA-GBM. Afterward, we evaluated the correlation between the highly expressed inhibitory ICs in the $CD8^+$ TILs of the included primary GBM, i.e., T cell immunoreceptor with Ig and ITIM domains

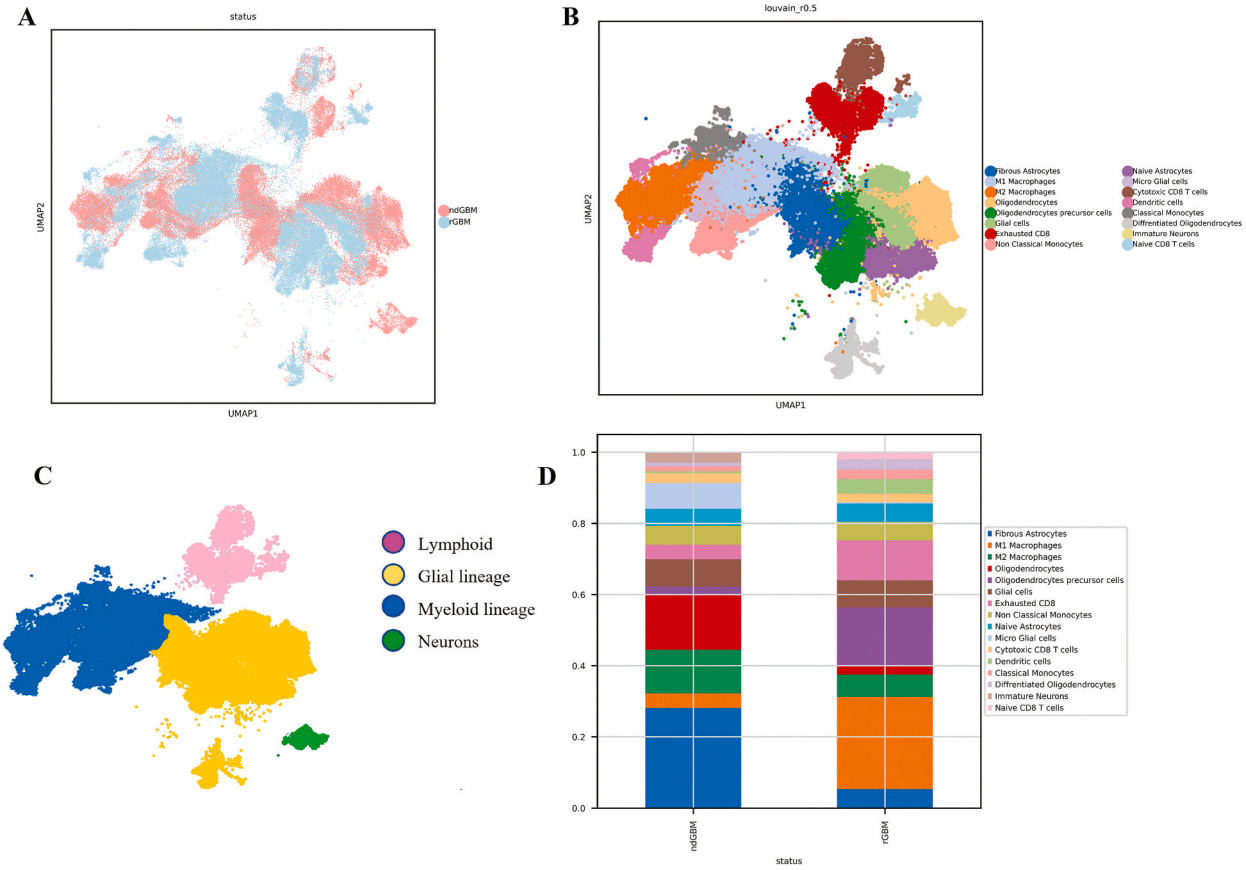

Fig. 1. Louvain clustering and identification of cell types within the TME of GBM were conducted for both primary (newly diagnosed = ndGBM) and recurrent (rGBM) cases. A) UMAP visualization was employed to display cells based on their status, whether they belonged to ndGBM or rGBM. B) UMAP representation was generated to illustrate the clustering of cells using Louvain clustering. Cells were annotated based on their canonical markers, and our in-depth analysis successfully identified 16 distinct clusters within the GBM TME. C) UMAP visualization was utilized based on the cell lineage of the identified cells. Cells were categorized into four distinguished lineages, providing insights into the diverse cellular origins within the GBM TME. D) A barplot was generated to depict the proportion of different cell types present in both ndGBM and rGBM statuses, offering a quantitative overview of the cellular composition in the primary and recurrent stages of GBM.

(*TIGIT*), with other relatively upregulated inhibitory ICs in the included primary GBM samples. Due to insufficient recurrent GBM sample count in TCGA-GBM, we accessed the CCGA platform (http://www.cgga.org.cn/) to study the correlational studies between the highly expressed inhibitory ICs in the $CD8^+$ TILs of the included recurrent GBM samples, i.e., cytotoxic T-lymphocyte–associated antigen 4 (*CTLA-4*), with other relatively upregulated inhibitory ICs in the included recurrent GBM tissues.

2.2.4. Statistical tests

In our study, rigorous statistical methods were employed to ensure the reliability and validity of our data analyses. Specifically, we utilized the Benjamini-Hochberg method to adjust p-values for DEG identification. This method is widely recognized for controlling the false discovery rate in multiple testing scenarios, enhancing the robustness of our findings. The adjusted p-values were crucial in minimizing the likelihood of false positives and, consequently, improving the overall accuracy of our DEG results. Furthermore, the Pearson correlation coefficient (R2) method was used in the gene-gene co-expression analyses. This method measures the linear association between two variables, in our case, gene expression levels. The Pearson correlation coefficient provides a quantitative measure of the strength and direction of the linear relationship between genes, allowing us to identify co-expression patterns. By utilizing this method, we aimed to uncover significant connections and interactions among genes, providing valuable insights into the regulatory networks within the biological system under investigation.

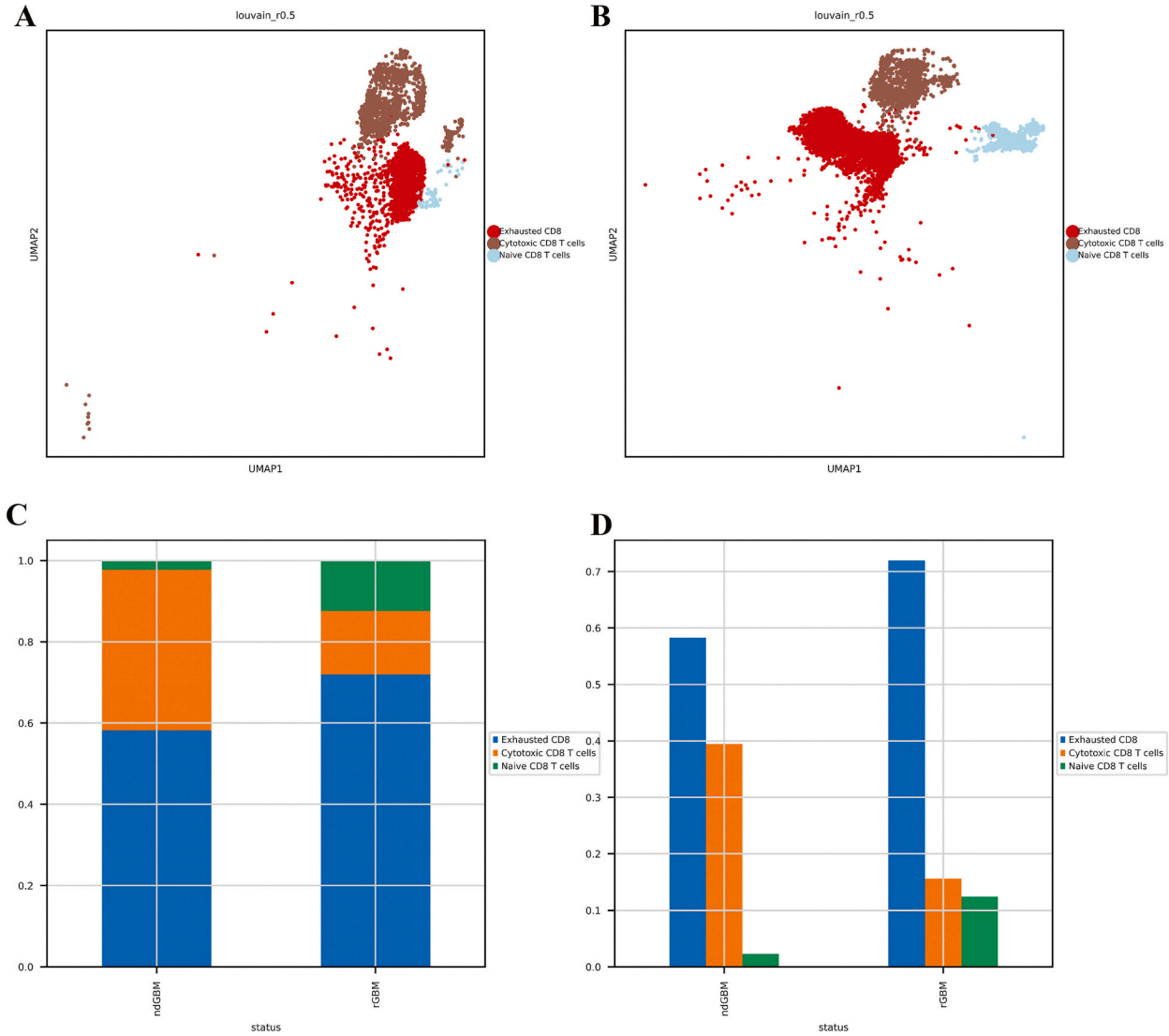

Fig. 2. Illustration of $CD8^+$ TILs subpopulations in both primary and recurrent GBM. A-B) UMAP visualizations of $CD8^+$ T cells, with A representing primary GBM cells and B representing recurrent GBM cells. C) Presentation of the ratio of $CD8^+$ TILs subpopulations in both primary and recurrent GBM cases. D) Representation of the frequency of $CD8^+$ TILs subpopulations in the included primary and recurrent GBM samples.

3. Results

3.1. Cell fractions could be different in the TME of the primary and recurrent GBM

After excluding low-quality cells, 107,395 cells were included in our single-cell RNA sequencing analyses. Cells were classified as originated from primary ($n = 56,592$; 53.7%) or recurrent GBM tissues ($n = 50,803$; 47.3%) (Fig. 1A). UMAP and unsupervised graph-based clustering partitioned cells into 16 clusters according to the expression of canonical gene markers in the primary and recurrent GBM (Fig. 1B). These clusters mainly belonged to four categories, i.e., neurons, glial, myeloid, and lymphoid cells (Fig. 1C). Fig. 1D depicts the cell-type percentages of included primary and recurrent GBM tissues. The results indicate that the cell-type profiles of primary and recurrent GBM can be different from each other.

3.2. Composition of CD8$^+$ TILs subpopulations in GBM TME: exhausted CD8$^+$ TILs have the majority of CD8$^+$ TILs of the primary and recurrent GBM

Computational analyses identified three distinct subpopulations of CD8$^+$ T-cells, i.e., naïve, cytotoxic, and exhausted cells (Fig. 2A and B). We found that naïve/memory CD8$^+$ T-cell signatures, i.e., C–C chemokine receptor type 7 (*CCR7*), interleukin-7 receptor (*IL7R*), transcription factor 7 (TCF7), selectin L (*SELL*), special AT-rich sequence-binding protein-1 (*SATB1*), G-protein coupled receptor 183 (*GPR183*), lymphotoxin beta (*LTB*), lymphoid enhancer-binding factor 1 (*LEF1*), and S100 calcium-binding protein A10 (*S100A10*), were highly expressed in naïve/memory subpopulations. Also, cytotoxic signatures, i.e., perforin 1 (*PRF1*), granzyme A (*GZMA*), Granzyme K (*GZMK*), and natural killer cell granule protein 7 (*NKG7*), showed the highest expression in cytotoxic CD8$^+$ T cell subpopulations. On the other hand, chemokine C-X-C motif ligand 13 (*CXCL13*), heat shock protein beta-1 (HSPB1), interferon regulatory factor 4 (*IRF4*), layilin (*LAYN*), GTPase IMAP family member 6 (*GIMAP6*), heat shock protein family H member 1 (*HSPH1*), C-X-C chemokine receptor type 6 (*CXCR6*), CTLA4, programmed cell death 1 (*PDCD1*), lymphocyte activation gene 3 (*LAG3*), hepatitis A virus cellular receptor 2 (*HAVCR2*), and TIGIT had the highest expression in the exhausted subpopulation. Our results showed a trend in which recurrent GBM samples display increased naïve/memory and exhausted CD8$^+$ TILs but reduced cytotoxic cells than primary GBM samples. We found that exhausted CD8$^+$ TILs had the majority of CD8$^+$ TILs in the included primary and recurrent tissues (Fig. 2C and D).

3.3. The expression pattern of inhibitory ICs in the CD8$^+$ TILs differs between primary GBM tissues

We subsequently investigated the hypothesis that the expression pattern of inhibitory ICs in CD8$^+$ TILs might have high heterogeneity at inter-tumoral levels in the included primary GBM samples. Our results indicated considerable inter-tumoral heterogeneity in

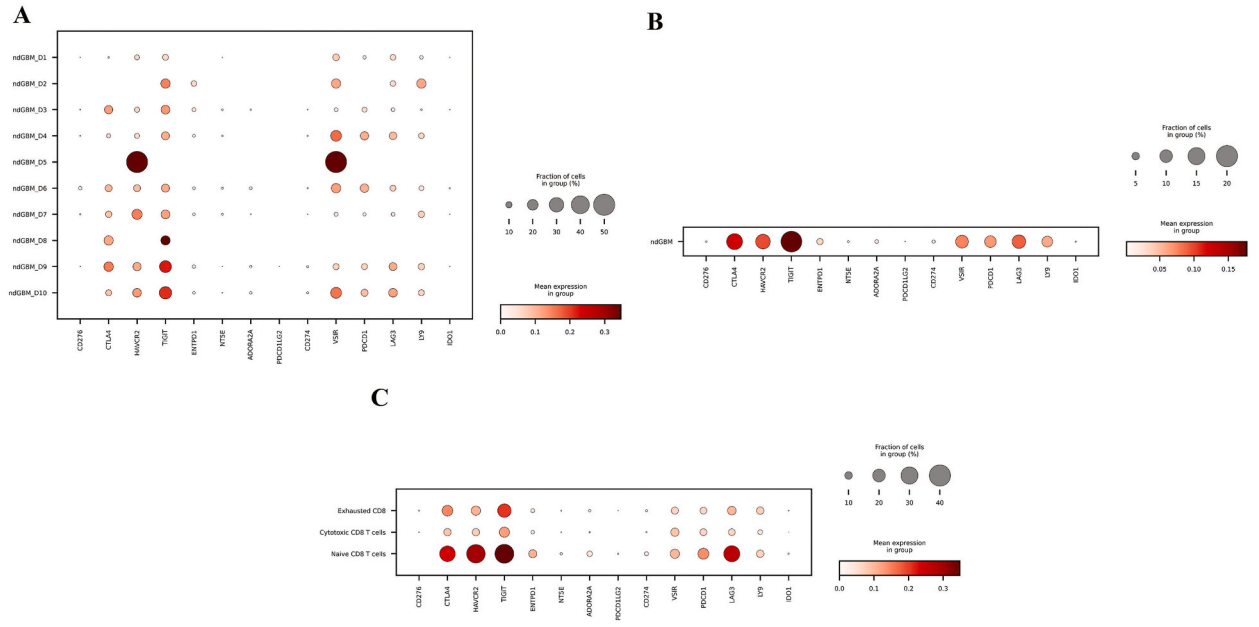

Fig. 3. The expression pattern of inhibitory IC molecules in CD8$^+$ TILs within the primary GBM samples. A) Dotplot demonstrates the inter-tumoral heterogeneity observed in the expression of inhibitory ICs within the CD8$^+$ TILs of the included primary GBM samples. B) Dotplot highlights the predominant expression of CTLA4, HAVCR2, TIGIT, VSIR, PDCD1, LAG3, and LY9 in the CD8$^+$ TILs of the included primary GBM samples. C) Dotplot indicates that inhibitory ICs were expressed to a minimal extent in the cytotoxic CD8$^+$ TILs in comparison to other subpopulations of CD8$^+$ TILs within the included primary GBM samples.

the expression of ICs in the CD8$^+$ TILs of primary GBM samples (Fig. 3A). We identified a trend in which *CTLA-4*, *HAVCR2*, *TIGIT*, V-Set immunoregulatory receptor (*VSIR)*, *PDCD1*, *LAG3*, and lymphocyte antigen 9 (*LY9*) expression were increased in the CD8$^+$ TILs of included primary GBM samples compared to other inhibitory ICs (Fig. 3B). Next, we studied the expression pattern of inhibitory ICs in the identified sub-populations of CD8$^+$ TILs in the included primary GBM samples (Fig. 3C). Compared with other CD8$^+$ T cell sub-populations, *CTLA-4*, *HAVCR2*, *TIGIT*, *PDCD1*, and *LAG3* were also widely expressed in the naïve/memory subpopulation (Fig. 3C). Interestingly, our results indicated a trend in which the studied inhibitory ICs had minimal expression in the cytotoxic CD8$^+$ TILs compared to other identified CD8$^+$ TILs subpopulations in the included primary GBM tissues (Fig. 3C).

3.4. Inhibitory ICs have a different expression pattern in the CD8$^+$ TILs of the included recurrent GBM tissues

We characterized the heterogeneity of inhibitory ICs expression of CD8$^+$ TILs at intra-tumoral, inter-tumoral, and subpopulation levels. Our results demonstrated high intra- and inter-tumoral heterogeneity in terms of the expression of the studied inhibitory ICs in the CD8$^+$ TILs of included recurrent GBM tissues (Fig. 4A). We identified a trend in which the CD8$^+$ TILs of included recurrent GBM tissues highly expressed *CTLA-4*, *TIGT*, *VISIR*, and *LAG3* compared to other studied inhibitory ICs (Fig. 4B). Furthermore, we analyzed the expression pattern of inhibitory ICs in the CD8$^+$ TILs subpopulations of included recurrent GBM samples. Compared with other CD8$^+$ TIL subpopulations, *CTLA-4*, *TIGIT, LAG3*, *VSIR*, and *PDCD1* were widely expressed in the exhausted subpopulation. In contrast, naïve/memory and cytotoxic subpopulations expressed these ICs at low levels (Fig. 4C). Of interest, our results indicated a trend in which most of the studied inhibitory ICs had decreased expression in the cytotoxic CD8$^+$ TILs subpopulation and increased expression in the exhausted CD8$^+$ TILs in the included recurrent GBM tissues (Fig. 4C).

3.5. Exhausted CD8$^+$ TILs cross-talk with other cells in the TME of primary and recurrent GBM

Because exhausted CD8$^+$ T-cells were the most dominant subpopulation of the CD8$^+$ TILs in the included primary and recurrent GBM samples, we investigated the cross-talk between exhausted CD8$^+$ TILs and other cells. Exhausted CD8$^+$ TILs had remarkable interactions with tumor-infiltrating dendritic cells in the included primary GBM TME (Fig. 5A). In the included primary GBM samples, the main signaling axis between tumor-infiltrating dendritic cells and exhausted CD8$^+$ TILs was mediated via the *CD99*/paired immunoglobin like type 2 receptor alpha (*PILRα*) axis (Fig. 5B). Likewise, we observed that exhausted CD8$^+$ TILs had considerable interactions with tumor-infiltrating dendritic cells in the included recurrent GBM tissues (Fig. 5C). In the included recurrent GBM samples, the main signaling axes between tumor-infiltrating dendritic cells and exhausted CD8$^+$ TILs were mediated via the HLA class I histocompatibility antigen, alpha chain E (*HLA-E*)/killer cell lectin-like receptor C3 (*KLRC3*), *HLA-E/*killer cell lectin-like receptor K1 (*KLRK1*), *HLA-E/*killer cell lectin-like receptor C2 (*KLRC2*), *HLA-E/*killer cell lectin like receptor C1(*KLRC1*), C-X-C motif chemokine ligand 12 (*CXCL12*)/CXC chemokine receptor 4 (*CXCR4*), neuregulin 1 (*NRG1*)/membrane spanning 4-domains A4A (*MS4A4A)*, CC-chemokine ligand 5 (*CCL5*)/C–C motif chemokine receptor 1 (*CCR1*), and macrophage migration inhibitory factor (*MIF*)/TNF receptor

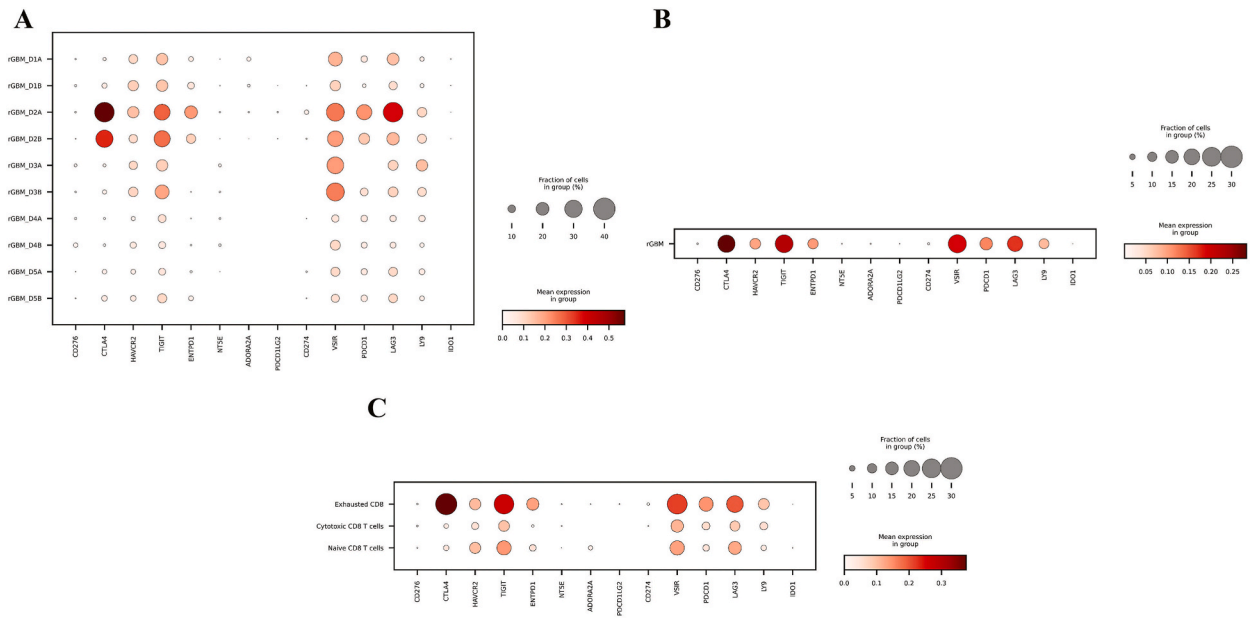

Fig. 4. Inhibitory IC expression pattern in the CD8$^+$ TILs of included recurrent GBM. A) Demonstrates both intra- and inter-tumoral variations in the inhibitory IC expression within CD8$^+$ TILs in the included recurrent GBM tissues. B) CTLA-4, TIGT, VISIR, and LAG3 exhibit predominant expression in the CD8$^+$ TILs of the included recurrent GBM tissues. C) The inhibitory ICs are notably elevated in exhausted CD8$^+$ TILs compared to other subpopulations of CD8$^+$ TILs in the included recurrent GBM samples.

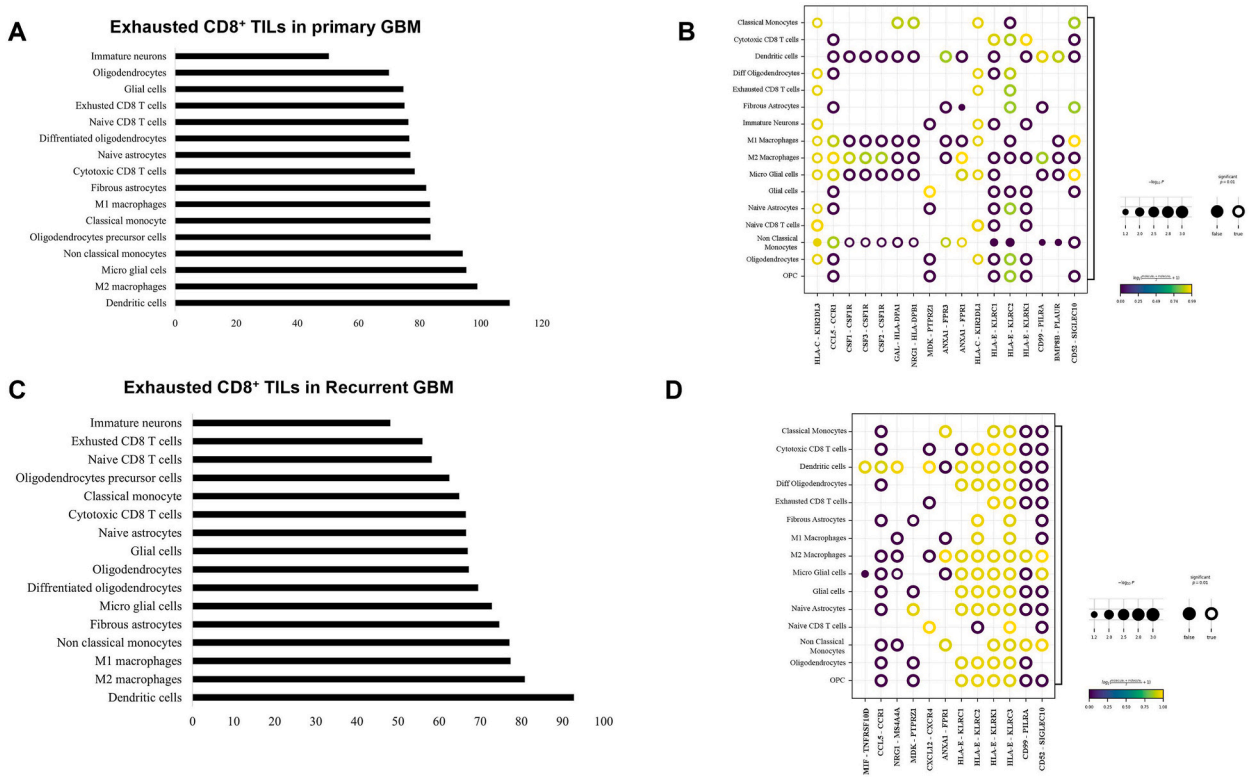

Fig. 5. The cross-talk between the exhausted CD8$^+$ TILs in the included primary and recurrent GBM. A) Exhausted CD8$^+$ TILs exhibit significant interactions with tumor-infiltrating dendritic cells in the primary GBM samples analyzed. B) The primary signaling axis between tumor-infiltrating dendritic cells and exhausted CD8$^+$ TILs may involve the CD99/PILRα axis in the primary GBM samples. C) Exhausted CD8$^+$ TILs display notable interactions with tumor-infiltrating dendritic cells in the recurrent GBM samples included in the study. D) The key signaling axis between tumor-infiltrating dendritic cells and exhausted CD8$^+$ TILs may be facilitated through HLA-E/KLRC3, HLA-E/KLRK1, HLA-E/KLRC2, HLA-E/KLRC1, CXCL12/CXCR4, NRG1/MS4A4A, CCL5/CCR1, and MIF/TNFRSF10D in the recurrent GBM samples analyzed. Fig. 6: Identifying DEGs and their molecular function. A) The volcano plot illustrates the DEGs in naïve/memory CD8$^+$ TILs. B) Molecular function enrichment analysis for the identified DEGs in naïve/memory CD8$^+$ TILs. C) The volcano plot showcases the DEGs in exhausted CD8$^+$ TILs. D) Molecular function enrichment analysis for the identified DEGs in exhausted CD8$^+$ TILs. E) The volcano plot displays the DEGs in cytotoxic CD8$^+$ TILs. F) Molecular function enrichment analysis for the identified DEGs in cytotoxic CD8$^+$ TILs. Red dots represent genes meeting predefined criteria, while blue dots indicate genes not meeting the criteria. (For interpretation of the references to colour in this figure legend, the reader is referred to the Web version of this article.)

superfamily member 10d (*TNFRSF10D)* axes (Fig. 5D).

3.6. DEG analysis of CD8$^+$ TILs subpopulations in the progression from primary to recurrent GBM

We studied the gene expression difference between the subpopulations of CD8$^+$ TILs in recurrent and primary GBM. We excluded pseudogenes, mitochondrially encoded, ribosomal, and RNA genes. In terms of naïve/memory CD8$^+$ TILs, histone H2A type 2-B (*HIST2H2AB*), histone H2B type 1-O (*HIST1H2BO*), major histocompatibility complex, class II, DQ alpha 2 (*HLA-DQA2)*, immunoglobulin lambda constant 1 (*IGLC1*), and histone H2B type 1-M (*HIST1H2BM)* were the top 5 significantly downregulated genes in recurrent GBM compared to primary GBM (Fig. 6A). thymosin beta 4 X-linked (*TMSB4X*), Fumarylacetoacetate Hydrolase (*FAH*), C-type lectin domain family 12 member A (*CLEC12A*), C-X-C motif chemokine ligand 3 (*CXCL3*), and Tetraspanin 13 (*TSPAN13*) were the top 5 significantly upregulated genes in the naïve/memory CD8$^+$ TILs of recurrent GBM compared to the naïve/memory CD8$^+$ TILs of primary GBM tissues (Fig. 6A). Fig. 6B demonstrates the molecular function enrichment of identified DEGs during the progression of naïve/memory CD8$^+$ TILs from primary GBM to recurrent GBM. The GSEA results have demonstrated that G2/M checkpoint and E2F-mediated cell cycle pathways are significantly more active in recurrent GBM naïve/memory CD8$^+$ than primary GBM ones (Supplementary Fig. 1A).

In exhausted CD8$^+$ TILs, *IGLC1*, phospholipase A2 group IIA (*PLA2G2A*), serpin family A member 3 (*SERPINA3)*, tissue factor pathway inhibitor 2 (*TFPI2*), and chromosome 6 open reading frame 141 (*C6orf141)* were the top 5 significantly downregulated genes in recurrent GBM compared to primary GBM samples (Fig. 6C). Interestingly, beta-2-microglobulin (*B2M*), *TMSB4X*, actin beta (*ACTB*), gamma-glutamyltransferase 1 (*GGT1*), and secreted frizzled-related protein 2 (*SFRP2)* were the top 5 significantly upregulated genes in the exhausted CD8$^+$ TILs of recurrent GBM compared to the exhausted CD8$^+$ TILs of primary GBM (Fig. 6C). Fig. 6D

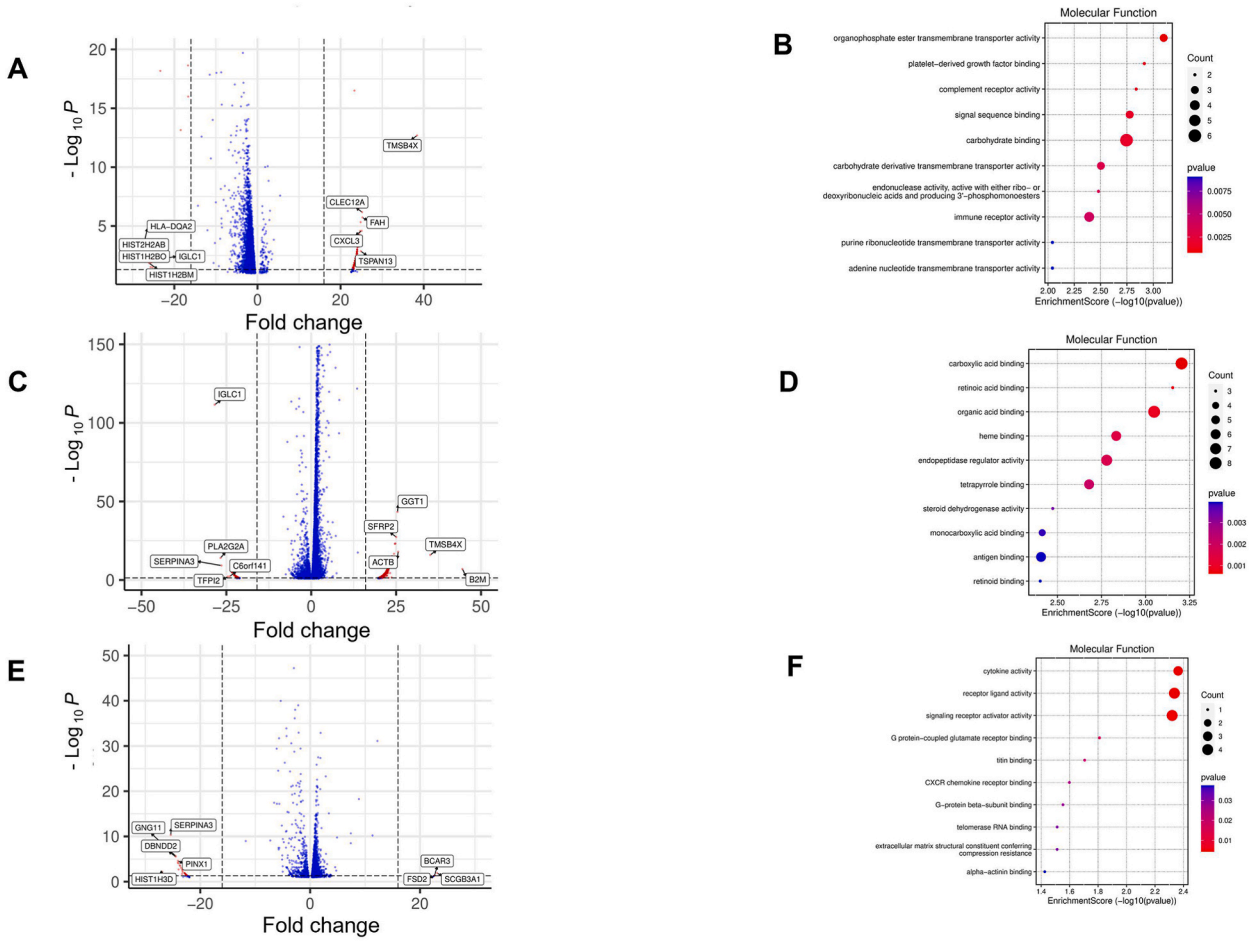

Fig. 6. Identifying DEGs and their molecular function. A) The volcano plot for identifying DEGs of naïve/memory CD8$^+$ TILs. B) Enrichment of the molecular function of the identified DEGs in naïve/memory CD8 + TILs. C) The volcano plot of DEGs of exhausted CD8+TILs. D) Enrichment of the molecular function of the identified DEGs in exhausted CD8$^+$ TILs. E) The volcano plot of DEGs of cytotoxic CD8$^+$ TILs. F) Enrichment of the molecular function of the identified DEGs in cytotoxic CD8$^+$ TILs. Red dots are genes that meet the predefined criteria, and blue dots are genes that do not meet the predefined criteria. (For interpretation of the references to colour in this figure legend, the reader is referred to the Web version of this article.)

displays the molecular function enrichment of identified DEGs during the progression of exhausted CD8$^+$ TILs from primary GBM to recurrent GBM. The GSEA results have shown that the tumor necrosis factor-alpha (TNF-α) via nuclear factor kappa B (NF-κB) and apoptosis pathways are significantly more active in recurrent GBM naïve/memory CD8$^+$ than primary GBM ones (Supplementary Fig. 1B).

In cytotoxic CD8$^+$ TILs, H3 clustered histone 4 (*HIST1H3D)*, *SERPINA3*, G protein subunit gamma 11 (*GNG11*), dysbindin domain containing 2 (*DBNDD2)*, and PIN2 (TERF1) Interacting Telomerase Inhibitor 1 (*PINX1*) were the top 5 significantly downregulated genes in recurrent GBM compared to primary GBM (Fig. 6E). Also, secretoglobin family 3A member 1 (*SCGB3A1*), breast cancer anti-estrogen resistance protein 3 (*BCAR3*), and fibronectin type III and SPRY domain containing 2 (*FSD2*) were the significantly upregulated genes in the cytotoxic CD8$^+$ TILs of recurrent GBM compared to primary GBM tissues (Fig. 6E). Fig. 6F shows the molecular function enrichment of identified DEGs during the progression of cytotoxic CD8$^+$ TILs from primary GBM to recurrent GBM.

4. Discussion

TME is crucial in determining the fate of various tumors [16,17]. This study was the first to thoroughly investigate the expression profile of three functional subpopulations of CD8$^+$ TILs in primary and recurrent GBM. Aside from *in-silico* findings, we provided the current evidence on the IC inhibitors in GBM, the reasons for the futility and side effects of their administration in the current method, and the significance of single-cell RNA sequencing in the cancer immunotherapy era. Besides, we provided the proof-of-concept and blueprint for future primary and recurrent GBM immunotherapy.

Cancer immunotherapy is a novel therapeutic approach that leverages the host's anti-tumoral immune responses to reject

malignant tumors. Accumulating evidence has highlighted the importance of immunosuppressive TME and the pathological expression of inhibitory ICs in attenuating anti-tumoral immune responses [3]. Following the pivotal roles of inhibitory ICs in cancer development, the related inhibiting mAbs have been developed against them. Although administrating one or two inhibitory IC blockades has improved some patients' survival, their overall beneficial effect on GBM patients has not been desirable. Blumenthal et al. have reported that administrating pembrolizumab, an anti-PD-1, has no clinical nor histological benefit for patients with primary brain tumors [18]. In recurrent GBM patients, the objective response rate (ORR) of pembrolizumab administration was 0% [19]. It was demonstrated that the ORR of recurrent GBM patients to nivolumab, another anti-PD-1, was 7.8% [9]. It was reported that the ORR of recurrent GBM patients on nivolumab was 3.8% [20], and the ORR of monotherapy with nivolumab was 11%, and its combination therapy with ipilimumab could not substantially increase the ORR in patients with recurrent GBMs [21]. Therefore, the current method of blocking inhibitory ICs is insufficient to bring meaningful clinical benefits to GBM patients.

Immune resistance development following the administration of one or two inhibitory IC blockades can be the reason for the undesirable response rate; tumor-intrinsic and tumor-extrinsic elements can be implicated in immune resistance following the administration of inhibitory IC inhibitors [22]. The upregulation of T-cell immunoglobulin and mucin domain-containing protein 3 (TIM-3) and other ICs can be the underlying reason for undesirable response to anti-PD-1 therapy, and the combined targeting of TIM-3 and PD-1 improves survival compared to monotherapy to anti-PD-1 [23]. Inhibiting CTLA-4, PD-1, or LAG3 leads to compensatory upregulation of other inhibitory ICs, facilitating immune resistance development and tumor growth [24]. Also, v-domain Ig suppressor of T cell activation (VISTA) upregulation following anti-PD-1 therapy can be the reason for the undesirable response rate of anti-PD-1 treatment [25]. A study has demonstrated that the expression levels of *CTLA-4* and *TIGIT* are remarkably increased in recurrent GBM treated with neoadjuvant anti-PD-1 therapy, indicating that the blockade of TIGIT and CTLA-4 along with PD-1 can increase the response rate of those patients [26]. Besides, TIGIT blockade can increase anti-PD-L1-mediated anti-tumoral immune responses [27,28]. TIGIT blockade can enhance the ability of anti-PD-1 treatment in terms of stimulating $CD8^+$ TILs-mediated anti-tumoral immune responses [29]. Consistent with this, a recent study has highlighted the negative impact of TIGIT on patients' survival and a positive association between PD-1 and TIGIT expression in tumor tissues [29]. Our results have indicated significant positive correlations between *TIGIT* with *CTLA-4*, *TIM-3*, *VISTA*, and *LAG3* in the tumor tissues of primary GBM patients (Supplementary Fig. 2). Our results have demonstrated significant positive correlations between *CTLA-4* with *TIGIT* and *LAG3* in the tumor tissues of recurrent GBM patients (Supplementary Fig. 3). Therefore, the dynamic nature of inhibitory IC expression requires targeting multiple inhibitory IC axes to liberate the TME from an immunosuppressive state.

Inhibitory IC blockade can impair physiological tolerance against normal tissues. VISTA knockdown paves the way for the T-helper-1/17 cells-mediated autoimmunity development [30], and the loss of VISTA can lead to cutaneous and systemic autoimmunity development in animal models [31]. Also, the co-deletion of PD-1 and LAG3 can lead to severe myocarditis in animal models [32]. It has been shown that loss of PD-1 or PD-L1 can increase insulin-specific follicular $CD4^+$ T-cells and increase autoantibody expression in animal models [33]. Aside from the stimulatory effect of inhibitory IC blockade on immune cells, the expression of inhibitory ICs can be substantially decreased in autoimmune conditions. For instance, *CTLA-4, PD-L1,* and *VISTA* expression levels are substantially downregulated in the peripheral blood monoclonal cells of multiple sclerosis patients compared to normal individuals [34,35]. Besides the pivotal role of inhibitory ICs in regulating immune responses and their decreased expression in autoimmune conditions, administrating inhibitory IC inhibitors in the current method can exacerbate autoimmunity. Growing reports have indicated that PD-1 and/or IDO1 blockade can increase the risk of autoimmunity development in GBM patients [36,37]. Also, a recent study has indicated that approximately 18% of GBM patients develop grade 3/4 of adverse events following anti-PD-1 treatment [9].

Single-cell sequencing technologies can be considered a milestone in our understanding of the expression profile of cells. It has been suggested that single-cell RNA sequencing can help us identify the inhibitory ICs' expression profile, which can be translated into the selection of related agents against them [12]. Durante has conferred that $CD8^+$ T-cells predominately express *LAG3* rather than *CTLA-4* and *PD-1* in uveal melanoma, and blocking LAG3 can be a potential therapeutic strategy for these patients [38]. A trend in which the expression of CD276 has been higher than CTLA-4 expression in included $CD45^+$ cells of recurrent GBM treated with pembrolizumab has been demonstrated [39]. Goswami et al. have identified a $CD73^{hi}$ macrophage subpopulation in GBM tissue that persists following anti-PD-1 therapy. They have shown that the loss of CD73 can substantially increase the survival of affected animals following anti-PD-1 and anti-CTLA-4 treatments [40]. Single-cell sequencing was applied on GBM tissues and demonstrated that following neoadjuvant anti-PD-1 treatment can augment TIGIT and CTLA-4 axes in GBM patients. It has been suggested that the blockade of these two inhibitory axes can improve the response rate of affected patients [26]. Therefore, the inhibitory IC blockade regiment should be tailored based on the inhibitory IC profile of the TME to minimize its side effects and increase its efficacy.

Following persistent exposure to foreign antigens, cytotoxic $CD8^+$ T-cells, developed from naïve/memory $CD8^+$ T-cells, become "exhausted." Besides, inhibitory ICs have essential roles in developing the exhausted state [7]. It has been indicated that the phenotype of $CD8^+$ TILs is a significant factor in determining GBM patients' prognosis [41]. Deng et al. have also demonstrated that *CTLA-4* expression increases following the transformation of cytotoxic $CD8^+$ TILs to exhausted $CD8^+$ TILs in melanoma tissues [6]. Single-cell RNA sequencing has also allowed us to study inhibitory IC expression on these three functional subgroups of $CD8^+$ TILs in the included primary and recurrent GBM tissues. Our results have shown a trend in which exhausted $CD8^+$ TILs express high levels of studied inhibitory ICs compared to other subpopulations in included recurrent GBM samples. Besides, *CTLA-4*, *TIGIT*, *CD39*, *VISTA*, *PD-1*, and *LAG3* have been notably expressed in the exhausted $CD8^+$ TILs of included recurrent GBM tissues. In the primary GBM samples, our results have demonstrated a trend in which cytotoxic $CD8^+$ TILs express low levels of studied inhibitory ICs compared to other subpopulations in the primary GBM samples. By categorizing $CD8^+$ T-cells into naïve, exhausted, and cytotoxic states, Kim et al. have shown that most of the exhausted $CD8^+$ T-cells are seen in tumor tissues, brain metastasis, and lymph node metastasis from lung tumors. However, cytotoxic $CD8^+$ T-cells have been abundant in normal lung tissues [42]. Also, most $CD8^+$ TILs are exhausted in

endometrial carcinoma [43]. The percentage of exhausted $CD8^+$ T-cells in the esophageal squamous carcinoma microenvironment is substantially higher than in adjacent normal tissues. Also, the infiltration of most active cytotoxic $CD8^+$ T-cells into the TME is substantially low [44]. We have shown that most $CD8^+$ TILs are exhausted $CD8^+$ TILs in the included primary and recurrent GBM tissues. Following the considerable presence of the exhausted $CD8^+$ TILs in the included primary and recurrent GBM tissues, we aimed to depict the cell interaction between exhausted $CD8^+$ TILs with other TME residing cells; exhausted $CD8^+$ TILs from included primary and recurrent GBM samples have high interactions with tumor-infiltrating dendritic cells. In the included primary GBM samples, the central signaling axis between tumor-infiltrating dendritic cells and exhausted $CD8^+$ TILs was mediated via the *CD99/PILRα* axis. The PILR family consists of two members, i.e., *PILRα* and *PILRβ*. *PILRα* possesses immunoreceptor tyrosine-based inhibitory motifs and mediates inhibitory response, while *PILRβ* possesses immunoreceptor tyrosine-based activation motifs and mediates the stimulatory response [45]. CD99 can be expressed in T-cells, and PILRα can be expressed in macrophages, dendritic cells, and granulocytes. The co-culture of PILR ligand with bone marrow-derived dendritic cells, which express PILRβ more than PILRα, can lead to increased expression of TNF-α and nitric oxide [46]. The *CXCL12/CXCR4* axis was one of the axes between tumor-infiltrating dendritic cells and exhausted $CD8^+$ TILs in recurrent GBM tissues. A single-cell RNA sequencing study in ovarian tumors indicated that *CXCR4* is highly expressed in $CD8^+$ T-cells. Besides, *CXCL12* has been highly expressed in interleukin 1-activated cancer-associated fibroblasts [47]. Consistent with this, CXCR4 was elevated in tumor-educated $CD8^+$ T-cells [48]. Benedicto et al. have reported that AMD3100, a CXCR4 antagonist, can substantially decrease tumor metastasis in animal models [49].

Furthermore, we investigated the differences in the gene expression of the naïve, exhausted, and cytotoxic $CD8^+$ TILs in primary and recurrent GBM tissues. We have shown that *SERPINA3* expression is substantially decreased in exhausted and cytotoxic $CD8^+$ TILs of recurrent GBM compared to their counterparts in primary GBM tissues. We have demonstrated that increased expression of *SERPINA3* is considerably associated with inferior survival in patients with recurrent GBM (Supplementary Fig. 5). SERPINA3 expression is upregulated in glioma tissues at mRNA and protein levels, and its expression is correlated with advanced tumor grade. The increased expression of *SERPINA3* is associated with the poor survival of low- and high-grade glioma patients [50]. Increased expression of *SERPINA3* is associated with the inferior overall survival and progression-free survival of GBM patients, and tumor-intrinsic *SERPINA3* is implicated in cell viability, cell cycle progression, tumor invasion, and cell migration of GBM cells. Besides, *SERPINA3* protein expression has been considerably higher in the infiltrating tumoral cells of the peritumoral brain zone [51]. Yuan et al. have reported a negative association between tumor-infiltrating $CD4^+$ T-cells and *SERPINA3* expression in glioma tissues [52]. Also, we have shown that *PLA2G2A* is substantially downregulated in the exhausted $CD8^+$ TILs of recurrent GBM compared to primary GBM tissues and *PLA2G2A* increased expression level is associated with poor survival of recurrent GBM patients (Fig. 6E and Supplementary Fig. 6). However, further studies are needed to study the biological effects of SERPINA3 and PLA2G2A in the mentioned $CD8^+$ TILs subpopulations in recurrent GBM.

Our study has some strengths: 1) we investigated $CD8^+$ TILs at a functional subpopulation scale both in primary and recurrent GBM; 2) we analyzed a panel of inhibitory ICs in $CD8^+$ TILs and related subpopulations and depicted a trend in their expression; 3) we characterized the difference between the $CD8^+$ TILs subpopulations in recurrent and primary GBM. 4) we investigated the cell-cell interaction between exhausted $CD8^+$ TILs and other TME-residing cells in primary and recurrent GBM. Nevertheless, our study has some limitations. Our analyses were not based on protein expression but on gene expression alone. Also, we could not experimentally investigate the function of identified DEGs and axes in the pertained $CD8^+$ TILs subpopulations. Overall, the current study substantially contributes to our understanding of GBM immunity and offers novel approaches to increase IC-based treatment efficacy for the affected patients.

5. Conclusion

The present study showed that the recurrent GBM samples display increased naïve/memory and exhausted $CD8^+$ TILs but reduced cytotoxic ones than primary GBM tissues. Exhausted $CD8^+$ TILs are the majority of $CD8^+$ TILs in the primary and recurrent GBM samples. There is vast inter-tumoral heterogeneity regarding inhibitory IC expression in the $CD8^+$ TILs of primary and recurrent GBM tissues. Cytotoxic $CD8^+$ TILs have minimal inhibitory IC expression both in the primary and recurrent GBM tissues. *CTLA-4* and *TIGIT* were highly expressed in the naïve/memory $CD8^+$ TILs of the primary GBM tissues and exhausted $CD8^+$ TILs of the recurrent GBM tissues. In both primary and recurrent GBM tissues, exhausted $CD8^+$ TILs have notable interactions with tumor-infiltrating dendritic cells; this cross-talk was mediated via the *CD99/PILRα* axis in the primary GBMs. However, this cross-talk was mediated via the *HLA-E/KLRC3*, *HLA-E/KLRK1*, *HLA-E/KLRC2*, *HLA-E/KLRC1*, *CXCL12/CXCR4*, *NRG1/MS4A4A*, *CCL5/CCR1*, and *MIF/TNFRSF10D* axes in recurrent GBMs.

Data statement

The dataset examined in this project may be found in the Gene Expression Omnibus (GEO) repository, specifically under the accession number GSE182109. The present work used the analyzed data from the Cancer Genome Atlas Glioblastoma Multiforme (TCGA-GBM) and Chinese Glioma Genome Atlas (CGGA).

Funding

None.

CRediT authorship contribution statement

Mahdi Abdoli Shadbad: Writing – original draft, Methodology, Conceptualization. **Adib Miraki Feriz:** Software, Investigation. **Behzad Baradaran:** Writing – review & editing. **Hossein Safarpour:** Writing – review & editing, Supervision, Software, Investigation.

Declaration of competing interest

The authors declare that they have no known competing financial interests or personal relationships that could have appeared to influence the work reported in this paper.

Acknowledgments

The research protocol was approved & Supported by Student Research Committee, Tabriz University of Medical Sciences (IR.TBZMED.VCR.REC.1401.255 and grant number: 70035). Parts of the graphical abstract were drawn using pictures from Servier Medical Art. Servier Medical Art by Servier is licensed under a Creative Commons Attribution 3.0 Unported License (https://creativecommons.org/licenses/by/3.0/).

Appendix A. Supplementary data

Supplementary data to this article can be found online at https://doi.org/10.1016/j.heliyon.2024.e27329.

References

[1] Y. Jiang, J. He, Y. Guo, H. Tao, F. Pu, YJJocb Li, Identification of genes related to low-grade glioma progression and prognosis based on integrated transcriptome analysis 121 (5–6) (2020) 3099–3111.
[2] M. Lechpammer, R. Rao, S. Shah, M. Mirheydari, D. Bhattacharya, A. Koehler, et al., Advances in immunotherapy for the treatment of adult glioblastoma, Overcoming Chemical and Physical Barriers 14 (7) (2022) 1627.
[3] N. Hosseinkhani, A. Derakhshani, O. Kooshkaki, M. Abdoli Shadbad, K. Hajiasgharzadeh, A. Baghbanzadeh, et al., Immune checkpoints and CAR-T cells: the pioneers in future cancer therapies? Int. J. Mol. Sci. 21 (21) (2020) 8305.
[4] J.M. Curtsinger, M.F. Mescher, Inflammatory cytokines as a third signal for T cell activation, Curr. Opin. Immunol. 22 (3) (2010) 333–340.
[5] H. Raskov, A. Orhan, J.P. Christensen, I. Gögenur, Cytotoxic CD8+ T cells in cancer and cancer immunotherapy, Br. J. Cancer 124 (2) (2021) 359–367.
[6] W. Deng, Y. Ma, Z. Su, Y. Liu, P. Liang, C. Huang, et al., Single-cell RNA-sequencing analyses identify heterogeneity of CD8+ T cell subpopulations and novel therapy targets in melanoma, Molecular Therapy-Oncolytics. 20 (2021) 105–118.
[7] W. Jiang, Y. He, W. He, G. Wu, X. Zhou, Q. Sheng, et al., Exhausted CD8+ T cells in the tumor immune microenvironment: new pathways to therapy, Front. Immunol. 11 (2021) 3739.
[8] N. Hosseinkhani, A. Derakhshani, M.A. Shadbad, A. Argentiero, V. Racanelli, T. Kazemi, et al., The role of V-domain Ig suppressor of T cell activation (VISTA) in cancer therapy: lessons learned and the road ahead, Front. Immunol. 12 (2021) 1797.
[9] D.A. Reardon, A.A. Brandes, A. Omuro, P. Mulholland, M. Lim, A. Wick, et al., Effect of nivolumab vs bevacizumab in patients with recurrent glioblastoma: the CheckMate 143 phase 3 randomized clinical trial, JAMA Oncol. 6 (7) (2020) 1003–1010.
[10] M. Abdoli Shadbad, N. Hemmat, V. Khaze Shahgoli, A. Derakhshani, F. Baradaran, O. Brunetti, et al., A systematic review on PD-1 blockade and PD-1 gene-editing of CAR-T cells for glioma therapy: from deciphering to personalized medicine, Front. Immunol. 12 (2021) 788211.
[11] N. Erfanian, A. Derakhshani, S. Nasseri, M. Fereidouni, B. Baradaran, N.J. Tabrizi, et al., Immunotherapy of cancer in single-cell RNA sequencing era: a precision medicine perspective, Biomed. Pharmacother. 146 (2022) 112558.
[12] A. Derakhshani, Z. Rostami, H. Safarpour, M.A. Shadbad, N.S. Nourbakhsh, A. Argentiero, et al., From oncogenic signaling pathways to single-cell sequencing of immune cells: changing the landscape of cancer immunotherapy, Molecules 26 (8) (2021) 2278.
[13] A. Miraki Feriz, F. Bahraini, A. Khosrojerdi, S. Azarkar, S.M. Sajjadi, E. HosseiniGol, et al., Deciphering the immune landscape of head and neck squamous cell carcinoma: a single-cell transcriptomic analysis of regulatory T cell responses to PD-1 blockade therapy, PLoS One 18 (12) (2023) e0295863.
[14] N. Erfanian, S. Nasseri, A. Miraki Feriz, H. Safarpour, M.H. Namaie, Characterization of Wnt signaling pathway under treatment of Lactobacillus acidophilus postbiotic in colorectal cancer using an integrated in silico and in vitro analysis, Sci. Rep. 13 (1) (2023) 22988.
[15] N. Abdelfattah, P. Kumar, C. Wang, J.-S. Leu, W.F. Flynn, R. Gao, et al., Single-cell analysis of human glioma and immune cells identifies S100A4 as an immunotherapy target, Nat. Commun. 13 (1) (2022) 1–18.
[16] R. Fasano, M.A. Shadbad, O. Brunetti, A. Argentiero, A. Calabrese, P. Nardulli, et al., Immunotherapy for hepatocellular carcinoma: new prospects for the cancer therapy, Life 11 (12) (2021) 1355.
[17] M.A. Shadbad, S. Safaei, O. Brunetti, A. Derakhshani, P. Lotfinejad, A. Mokhtarzadeh, et al., A systematic review on the therapeutic potentiality of PD-L1-inhibiting MicroRNAs for triple-negative breast cancer: toward single-cell sequencing-guided biomimetic delivery, Genes 12 (8) (2021) 1206.
[18] D.T. Blumenthal, M. Yalon, G.W. Vainer, A. Lossos, S. Yust, L. Tzach, et al., Pembrolizumab: first experience with recurrent primary central nervous system (CNS) tumors, J. Neuro Oncol. 129 (3) (2016) 453–460.
[19] L. Nayak, A.M. Molinaro, K. Peters, J.L. Clarke, J.T. Jordan, J. de Groot, et al., Randomized phase II and biomarker study of pembrolizumab plus bevacizumab versus pembrolizumab alone for patients with recurrent glioblastoma, Clin. Cancer Res. 27 (4) (2021) 1048–1057.
[20] T. Aoki, N. Kagawa, K. Sugiyama, T. Wakabayashi, Y. Arakawa, S. Yamaguchi, et al., Efficacy and safety of nivolumab in Japanese patients with first recurrence of glioblastoma: an open-label, non-comparative study, Int. J. Clin. Oncol. 26 (12) (2021) 2205–2215.
[21] A. Omuro, G. Vlahovic, M. Lim, S. Sahebjam, J. Baehring, T. Cloughesy, et al., Nivolumab with or without ipilimumab in patients with recurrent glioblastoma: results from exploratory phase I cohorts of CheckMate 143, Neuro Oncol. 20 (5) (2018) 674–686.
[22] B. Zhou, Y. Gao, P. Zhang, Q. Chu, Acquired resistance to immune checkpoint blockades: the underlying mechanisms and potential strategies, Front. Immunol. 12 (2021).
[23] S. Koyama, E.A. Akbay, Y.Y. Li, G.S. Herter-Sprie, K.A. Buczkowski, W.G. Richards, et al., Adaptive resistance to therapeutic PD-1 blockade is associated with upregulation of alternative immune checkpoints, Nat. Commun. 7 (1) (2016) 1–9.
[24] R.-Y. Huang, A. Francois, A.R. McGray, A. Miliotto, K. Odunsi, Compensatory upregulation of PD-1, LAG-3, and CTLA-4 limits the efficacy of single-agent checkpoint blockade in metastatic ovarian cancer, OncoImmunology 6 (1) (2017) e1249561.

[25] H. Kakavand, L.A. Jackett, A.M. Menzies, T.N. Gide, M.S. Carlino, R.P. Saw, et al., Negative immune checkpoint regulation by VISTA: a mechanism of acquired resistance to anti-PD-1 therapy in metastatic melanoma patients, Mod. Pathol. 30 (12) (2017) 1666–1676.
[26] A.H. Lee, L. Sun, A.Y. Mochizuki, J.G. Reynoso, J. Orpilla, F. Chow, et al., Neoadjuvant PD-1 blockade induces T cell and cDC1 activation but fails to overcome the immunosuppressive tumor associated macrophages in recurrent glioblastoma, Nat. Commun. 12 (1) (2021) 1–16.
[27] R.J. Johnston, L. Comps-Agrar, J. Hackney, X. Yu, M. Huseni, Y. Yang, et al., The immunoreceptor TIGIT regulates antitumor and antiviral CD8+ T cell effector function, Cancer Cell 26 (6) (2014) 923–937.
[28] T. Inozume, T. Yaguchi, J. Furuta, K. Harada, Y. Kawakami, S. Shimada, Melanoma cells control antimelanoma CTL responses via interaction between TIGIT and CD155 in the effector phase, J. Invest. Dermatol. 136 (1) (2016) 255–263.
[29] N. Hosseinkhani, M.A. Shadbad, M. Asghari Jafarabadi, N. Karim Ahangar, Z. Asadzadeh, S.M. Mohammadi, et al., A systematic review and meta-analysis on the significance of TIGIT in solid cancers: dual TIGIT/PD-1 blockade to overcome immune-resistance in solid cancers, Int. J. Mol. Sci. 22 (19) (2021) 10389.
[30] L. Wang, I. Le Mercier, J. Putra, W. Chen, J. Liu, A.D. Schenk, et al., Disruption of the immune-checkpoint VISTA gene imparts a proinflammatory phenotype with predisposition to the development of autoimmunity, Proc. Natl. Acad. Sci. USA 111 (41) (2014) 14846–14851.
[31] X. Han, M.D. Vesely, W. Yang, M.F. Sanmamed, T. Badri, J. Alawa, et al., PD-1H (VISTA)–mediated suppression of autoimmunity in systemic and cutaneous lupus erythematosus, Sci. Transl. Med. 11 (522) (2019) eaax1159.
[32] T. Okazaki, I-m Okazaki, J. Wang, D. Sugiura, F. Nakaki, T. Yoshida, et al., PD-1 and LAG-3 inhibitory co-receptors act synergistically to prevent autoimmunity in mice, J. Exp. Med. 208 (2) (2011) 395–407.
[33] T. Martinov, L.A. Swanson, E.R. Breed, C.G. Tucker, A.J. Dwyer, J.K. Johnson, et al., Programmed death-1 restrains the germinal center in type 1 diabetes, J. Immunol. 203 (4) (2019) 844–852.
[34] A. Derakhshani, Z. Asadzadeh, H. Safarpour, P. Leone, M.A. Shadbad, A. Heydari, et al., Regulation of ctla-4 and pd-l1 expression in relapsing-remitting multiple sclerosis patients after treatment with fingolimod, ifnβ-1α, glatiramer acetate, and dimethyl fumarate drugs, J. Personalized Med. 11 (8) (2021) 721.
[35] A. Derakhshani, Z. Asadzadeh, B. Baradaran, H. Safarpour, S. Rahmani, P. Leone, et al., The expression pattern of VISTA in the PBMCs of relapsing-remitting multiple sclerosis patients: a single-cell RNA sequencing-based study, Biomed. Pharmacother. 148 (2022) 112725.
[36] R. Thummalapalli, T. Heumann, J. Stein, S. Khan, D.S. Priemer, A.S. Duffield, et al., Hemophagocytic lymphohistiocytosis secondary to PD-1 and Ido inhibition in a patient with refractory glioblastoma, Case Rep. Oncol. 13 (2) (2020) 508–514.
[37] M. Simonelli, L. Di Tommaso, M. Baretti, A. Santoro, Pathological characterization of nivolumab-related liver injury in a patient with glioblastoma, Immunotherapy 8 (12) (2016) 1363–1369.
[38] M.A. Durante, D.A. Rodriguez, S. Kurtenbach, J.N. Kuznetsov, M.I. Sanchez, C.L. Decatur, et al., Single-cell analysis reveals new evolutionary complexity in uveal melanoma, Nat. Commun. 11 (1) (2020) 1–10.
[39] J. De Groot, M. Penas-Prado, K. Alfaro-Munoz, K. Hunter, B.L. Pei, B. O'Brien, et al., Window-of-opportunity clinical trial of pembrolizumab in patients with recurrent glioblastoma reveals predominance of immune-suppressive macrophages, Neuro Oncol. 22 (4) (2020) 539–549.
[40] S. Goswami, T. Walle, A.E. Cornish, S. Basu, S. Anandhan, I. Fernandez, et al., Immune profiling of human tumors identifies CD73 as a combinatorial target in glioblastoma, Nat. Med. 26 (1) (2020) 39–46.
[41] M. Abdoli Shadbad, Z. Asadzadeh, N. Hosseinkhani, A. Derakhshani, N. Alizadeh, O. Brunetti, et al., A systematic review of the tumor-infiltrating CD8+ T cells/PD-L1 axis in high-grade glial tumors: toward personalized immuno-oncology, Front. Immunol. (2021) 3830.
[42] N. Kim, H.K. Kim, K. Lee, Y. Hong, J.H. Cho, J.W. Choi, et al., Single-cell RNA sequencing demonstrates the molecular and cellular reprogramming of metastatic lung adenocarcinoma, Nat. Commun. 11 (1) (2020) 1–15.
[43] Y-e Guo, Y. Li, B. Cai, Q. He, G. Chen, M. Wang, et al., Phenotyping of immune and endometrial epithelial cells in endometrial carcinomas revealed by single-cell RNA sequencing, Aging (Albany NY) 13 (5) (2021) 6565.
[44] Y. Zheng, Z. Chen, Y. Han, L. Han, X. Zou, B. Zhou, et al., Immune suppressive landscape in the human esophageal squamous cell carcinoma microenvironment, Nat. Commun. 11 (1) (2020) 1–17.
[45] D.D. Mousseau, D. Banville, D. L'Abbé, P. Bouchard, S.-H. Shen, PILRα, a novel immunoreceptor tyrosine-based inhibitory motif-bearing protein, recruits SHP-1 upon tyrosine phosphorylation and is paired with the truncated counterpart PILRβ, J. Biol. Chem. 275 (6) (2000) 4467–4474.
[46] I. Shiratori, K. Ogasawara, T. Saito, L.L. Lanier, H. Arase, Activation of natural killer cells and dendritic cells upon recognition of a novel CD99-like ligand by paired immunoglobulin-like type 2 receptor, J. Exp. Med. 199 (4) (2004) 525–533.
[47] M. Hornburg, M. Desbois, S. Lu, Y. Guan, A.A. Lo, S. Kaufman, et al., Single-cell dissection of cellular components and interactions shaping the tumor immune phenotypes in ovarian cancer, Cancer Cell 39 (7) (2021) 928–944. e6.
[48] Y.-N. Lin, M.O. Schmidt, G.M. Sharif, E.E. Vietsch, A.J. Kiliti, M.E. Barefoot, et al., Impaired CXCL12 signaling contributes to resistance of pancreatic cancer subpopulations to T cell-mediated cytotoxicity, OncoImmunology 11 (1) (2022) 2027136.
[49] A. Benedicto, I. Romayor, B. Arteta, CXCR4 receptor blockage reduces the contribution of tumor and stromal cells to the metastatic growth in the liver, Oncol. Rep. 39 (4) (2018) 2022–2030.
[50] D. Luo, W. Chen, Y. Tian, J. Li, X. Xu, C. Chen, et al., Serpin peptidase inhibitor, clade A member 3 (SERPINA3), is overexpressed in glioma and associated with poor prognosis in glioma patients, OncoTargets Ther. 10 (2017) 2173.
[51] V.P. Nimbalkar, B.S. Kruthika, P. Sravya, S. Rao, H.S. Sugur, B.K. Verma, et al., Differential gene expression in peritumoral brain zone of glioblastoma: role of SERPINA3 in promoting invasion, stemness and radioresistance of glioma cells and association with poor patient prognosis and recurrence, J. Neuro Oncol. 152 (1) (2021) 55–65.
[52] Q. Yuan, S.Q. Wang, G.T. Zhang, J. He, Z.D. Liu, M.R. Wang, et al., Highly expressed of SERPINA3 indicated poor prognosis and involved in immune suppression in glioma, Immunity, Inflammation and Disease 9 (4) (2021) 1618–1630.